Broadband delay lines and nonreciprocal resonances in unidirectional waveguides

Sander A. Mann, Dimitrios L. Sounas, and Andrea Alù

Phys. Rev. B **100**, 020303 — Published 24 July 2019

DOI: 10.1103/PhysRevB.100.020303

Broadband delay lines and nonreciprocal resonances in unidirectional waveguides

Sander A. Mann[1,2], Dimitrios L. Sounas[2,5], and Andrea Alù[1,2,3,4,*]

[1]*Photonics Initiative, Advanced Science Research Center, City University of New York, New York 10031, USA*

[2]*Department of Electrical and Computer Engineering, The University of Texas at Austin, Austin, TX, USA*

[3]*Physics Program, Graduate Center, City University of New York, New York 10016, USA*

[4]*Department of Electrical Engineering, City College of The City University of New York, New York 10031, USA*

[5]*Department of Electrical and Computer Engineering, Wayne State University, Detroit, MI 48202, USA*

**aalu@gc.cuny.edu*

Slow-light waveguides play an important role in optical pulse delay lines, but are practically limited by disorder-induced attenuation. Topological edge states, unidirectional and robust against disorder, have been proposed as a way to address this issue. Here, we study the transmission phase and pulse propagation dynamics through unidirectional systems in the presence of strong discontinuities. We first investigate a magnetically-biased slow-light channel, demonstrating broadband pulse delays in small footprints. We uncover a novel nonreciprocal etalon-like resonance, sustained by propagating forward and evanescent backward modes, affecting pulse propagation and delay. We then show the existence of these features in topologically protected edge states, highlighting their universality. These exotic resonances provide a new degree of freedom in unidirectional waveguides to engineer their response, and they may therefore prove highly useful in various nanophotonic applications.

Compact delay lines are highly desirable for integrated photonic signal processing. To date, they are most commonly pursued through structured slow light [1–3]. Unfortunately, both fundamental and practical constraints limit how compact and broadband a delay line can be. Fundamentally, the minimum footprint is bound by the group delay and pulse bandwidth, through the so-called delay-bandwidth limit [4]. Practically, the low group velocities and associated high field intensities in these delay lines make them sensitive to disorder [5,6], leading to backscattering and reduced transmission. Additionally, intricate (adiabatic) matching regions are required to achieve low group velocities over wide bandwidths, increasing complexity and footprint [7]. Recently, topological photonic insulators have been suggested as a solution to these practical issues: they support robust unidirectional edge states that maintain transmission despite strong perturbations or abrupt transitions [8–10]. It has been shown that a slow light transmission window across a topologically non-trivial bandgap can be maintained even in the presence of strong disorder [11], and that delays can be achieved by simply using sharp corners to fold up the waveguide, reducing the overall footprint [12]. However, the impact of discontinuities, disorder and impedance matching on transmission phase in one-way and topological waveguides has not been thoroughly studied, even though this aspect is at least equally important for the successful implementation of unidirectional technologies.

Here, we study pulse propagation through unidirectional waveguides in the presence of perturbations and discontinuities in model systems at THz and GHz frequencies. We investigate the role of boundaries between fast and slow light regions in a canonical unidirectional delay line formed by a one-way plasmonic waveguide, demonstrating broadband pulse delays in an extremely small footprint. We show that the

junctions do not reflect, as expected, but that they do play a crucial role in the total group delay of the system. We elucidate their role using an equivalent model that accurately describes the total delay line, based on temporal coupled-mode theory for nonreciprocal systems that we have recently developed [13]. We find that one-way structures are in general able to support a new type of resonance, similar to resonances in Gires-Tournois (GT) or Fabry-Pérot (FP) etalons, but now comprising a unidirectional medium. Finally, we demonstrate how these features arise also in topologically protected edge states between two photonic crystals with different band structure topologies, generalizing our findings to the broad class of topological photonic systems.

Consider first the canonical two-dimensional slow light waveguide formed by a plasmonic "metal" (a narrowband semiconductor InSb at THz frequencies, due to free carriers [14]) in close proximity to a perfect electric conductor (PEC), with a small dielectric spacer in between. For thin dielectric layers this waveguide supports a single surface-plasmon polariton (SPP), identical to the lowest order mode in a metal-insulator-metal (MIM) waveguide due to symmetry conditions imposed by the PEC [15–18]. Plasmonic MIM waveguides are an excellent platform to study broadband slow light, as with small dielectric thicknesses the group velocity becomes extremely small over a large bandwidth [19]. This is confirmed in Fig. 1a, which shows the real part of the propagation constant for a 12 and 0.12 μm thick Si layer normalized to the wavenumber at the plasma frequency k_p (blue and red dashed lines respectively, see [20] for details on the geometries). We only show $\Re(k)$ up to the frequency where the mode becomes evanescent.

When the metal is biased with a static magnetic field, its permittivity becomes gyrotropic, resulting in nonreciprocal SPP dispersion [21–25]. Fig. 1a shows the dispersion of the same two waveguides, but now with a magnetic bias $\mathbf{B} = -0.25\hat{\mathbf{z}}\,\mathrm{T}$ (solid lines) transverse to the direction of propagation. The left-right symmetry is broken and, crucially, the asymptote in the forward ($+\hat{x}$) direction moves to higher frequencies, while the backward asymptote shifts to lower frequencies. This opens a frequency range where the SPP only propagates in the forward direction (shown in gray shading in Fig. 1a). Furthermore, as with the reciprocal MIM waveguide, the group velocity v_g within the unidirectional frequency range strongly depends on the dielectric layer thickness. Going from 12 to 0.12 μm dielectric thickness, the group velocity is significantly reduced over the whole range (by a factor of 49.8 at 1.5 THz), enabling broadband, unidirectional slow waves. The proximity of the PEC ensures that the SPP is the only propagating mode, and as a result propagation is reflection-free, even in the presence of very strong scatterers [22,23,26–29].

We make use of such unidirectional and broadband slow light features to form compact, broadband delay lines. Despite the large change in momentum and group index between the thicker and thinner waveguides, we can simply connect the narrow section to the wider waveguide, as schematically shown in Fig. 1b, without worrying about mismatch and reflections. Since the waveguide is translation invariant in the $\hat{z}$-direction (and $k_z = 0$), it is effectively two-dimensional. Because there are no propagating modes in the backward direction there is no need for matching architectures, and, in the absence of absorption, full transmission is guaranteed. As a first example, we take a 10 μm long delay line (1/20$^{\text{th}}$ of the free space wavelength $\lambda_0 = 200\ \mu\mathrm{m}$) consistent with the geometry in Fig.

1b, and numerically calculate the transfer function $t(\omega)$ between the input and output junctions (using an overlap integral for nonreciprocal systems [30]), from which we can retrieve the propagated pulse and the group delay τ_g [20]. Fig. 1c shows the input pulse ($f_0 = 1.5\ \text{THz}, \Delta f = f_0 / 8\ \text{THz}$) in blue, and for comparison we also show the pulse after propagating over 10 μm in the thick waveguide (orange, dashed). The group delay $\tau_g = 0.55\,\text{ps}$ is negligible compared to the pulse width. In stark contrast, the pulse at the output plane of the delay line is shown as the solid orange line, and the group delay has increased to $\tau = 29.7\ \text{ps}$, more than the temporal bandwidth of the pulse itself, an increase by a factor of 54 compared to the wide waveguide over the same distance.

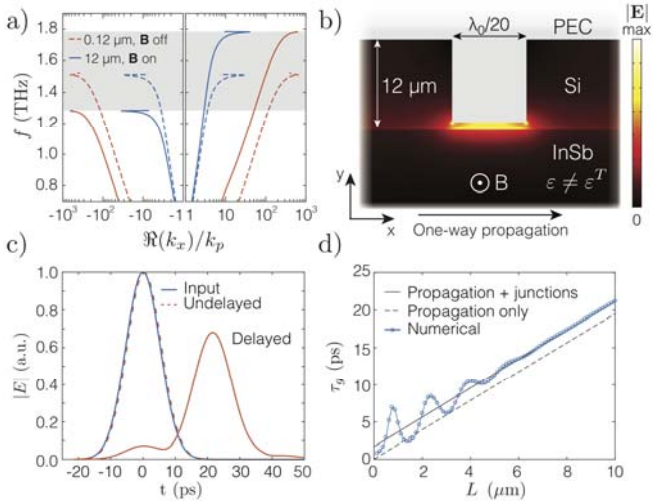

Fig. 1: a) Dispersion of InSb-Si-PEC waveguides with 12 μm Si (blue) and 0.12 μm Si spacer (red), with and without magnetic bias **B** perpendicular to the direction of propagation (solid and dashed, respectively). With **B** there is a unidirectional frequency range, shown in gray. b) Schematic depiction of a compact unidirectional plasmonic delay line without matching regions. c) Comparison of pulse delay without (orange dashed) and with (orange solid) reduction of the dielectric thickness as shown in b), demonstrating significant delay. d) Peak-to-peak delay as a function of delay line length for the geometry shown in b). With respect to the expected propagation delay (black dashed line), we observe a vertical offset (black solid line) and oscillations for small lengths.

Interestingly, the increase in group delay between the wide waveguide and the delay line exceeds the expected group delay based on the group velocity increase by 8% (the ratio was 49.8). This discrepancy persists for other delay line lengths as well, as shown in Fig. 1d: the expected group delay is shown by the dashed black line, while the actual group delay obtained from numerical simulations is shown by the blue dots. In fact, we observe two distinct effects: 1) a constant offset, even for vanishing delay line length, and 2) an oscillation in the group delay that decreases in amplitude for longer delay line lengths. The two effects arise for other Si layer thicknesses as well: we present the same analysis for a 1 μm thick Si layer delay line in [20]. To understand these phenomena, we must explicitly

take the role of the waveguide junctions into account: even though the abrupt junctions do not lead to reflections due to unidirectionality, they do appear to play a significant role in the dynamics of the unidirectional delay line.

We start by considering only the first junction, between the fast and slow waveguide. This transition is decidedly diabatic, exciting strong evanescent fields in the process (see Fig. 1b for an exemplary field intensity plot). These evanescent fields at the junction are responsible for stored (reactive) energy W_X at the junctions, which, in the ideal case of nondispersive materials and full transmission, is known to lead to a junction-induced group delay $\tau_j = W_X / P_{in}$ [31]. More generally, we can calculate the group delay directly from the transmission coefficient $t_1(\omega)$ of the junction: $\tau_{j,1} = -\partial \arg(t_1(\omega)) / \partial \omega$. Doing so yields a group delay at 1.5 THz of $\tau_{1,j} = 0.85$ ps [20]. Interestingly, we have previously shown that the transmission coefficient of the second junction $t_2(\omega)$ is identical to $t_1(\omega)$ ($\tau_{j,2} = \tau_{j,1} = \tau_j$, confirmed numerically [20]), because the second junction is the time-reversed version of the first one [13]. Adding the temporal delay due to the two junctions to the group delay originating from propagation in the narrow waveguide itself, we find the solid black line in Fig. 1d. The actual group delay clearly asymptotes towards τ_0 for long delay lines, evidencing the temporal contributions of the junctions.

To explain the oscillatory response for short lengths, we need to additionally consider that the junctions are not only connected through the propagating mode in the delay line, but for short distances they are also connected evanescently through higher-order evanescent modes. To capture the dynamics of the total system, we construct an equivalent model of the full delay line [32,33]. For simplicity, we treat the reactance of both

junctions as a detuned nonreciprocal resonance, capturing the stored reactive energy around the junctions, which allows us to use previously derived identities for such coupled resonant systems [13], considerably simplifying our analysis. It should be emphasized, however, that these junctions are not really resonators, and that the equivalent representation is appropriate only over a finite spectral window around the frequency of interest.

Starting with an equivalent description of the single junction, the equation of motion reads

$$\frac{d}{dt}X = (i\omega_0 - \gamma)X + ks_+, \tag{1}$$

where X is a complex amplitude normalized so that $W_X = |X|^2$ is the stored energy in the near field of the junction, ω_0 is the resonant frequency, γ is the decay rate, and k is the in-coupling coefficient relating the driving term s_+ to the amplitude X. The driving term is normalized so that $|s_+|^2$ is the input power. The transmitted amplitude past the junction is given by

$$s_- = Cs_+ + dX = C\left(1 - \frac{2\gamma}{i(\omega_0 - \omega) - \gamma}\right)s_+, \tag{2}$$

where C is the direct transmission coefficient and d is the outcoupling coefficient, relating the transmitted amplitude to X. In deriving Eq. (2), we have used $|d|^2 = 2\gamma$, and the nonreciprocal identity $Cd^* = -k$ [13]. We find the modeled delay to be equal to the one of a non-dispersive, fully transmitting junction [20,31]. The model parameters C, γ and ω_0 are extracted directly from the numerically calculated transmission coefficient, and the model obtains good agreement with the numerical transfer function [20].

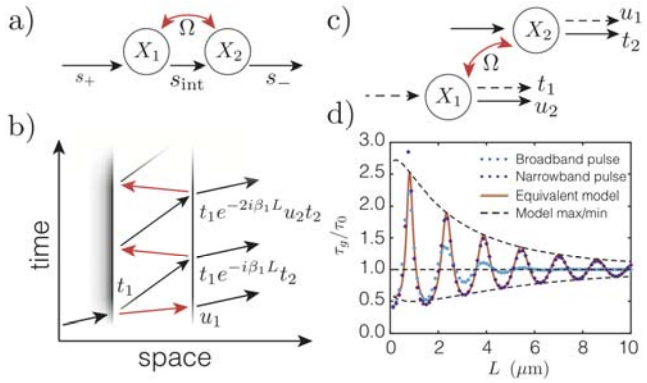

Fig. 2: a) Schematic of how the two junctions are connected, both through the unidirectional channel (black arrow) and evanescently (red arrow). b) Etalon-like depiction of the interaction between the junctions, where red shows evanescent processes u_1 (right arrow) and u_2 (left arrow). c) Schematic depiction of how the transmission and coupling amplitudes in b) are determined [20], when X_1 or X_2 is excited (dashed or solid line respectively). d) Relative enhancement predicted by the equivalent model, compared to numerical results for two pulse bandwidths, including maximum possible deviation.

Armed with this accurate model of the single junction, we can move forward to model the total delay line, where we consider that the second junction is driven by the output of the fist junction as well as evanescent coupling between the junctions (shown schematically at the top of Fig. 2a with the red arrow). Instead of solving the corresponding system of equations directly (as discussed in [20]), we follow an equivalent but more insightful approach: we treat the coupled resonators as an etalon (Fig. 2b), where each reactance is treated as an interface that may transmit into the next waveguide section or evanescently couple to the waveguide section following the other reactance ($t_{1,2}$ and $u_{1,2}$, respectively, see Fig. 2c for a schematic and [20] for expressions of these coefficients). These amplitudes thus correspond to a system where X_2 is not driven by the output of X_1, but by a different input waveguide. The total transmission coefficient for the full system is then calculated by

summing all wave amplitudes in the output waveguide, as shown for the first three in Fig. 2b. This summation results in

$$t = u_1 + \frac{t_1^2 e^{-i\beta_1 L}}{1 - u_2 e^{-i\beta_1 L}}, \tag{3}$$

where we have used the fact that $t_1 = t_2$ (due to time-reversal symmetry [13]), and where β_1 is the wavenumber of the propagating mode. $t_{1,2}$ and $u_{1,2}$ depend on the length-dependent coupling strength Ω between the two junctions, which we determine by expressing it as a sum of evanescent modes, $\Omega(L) = \sum C_n e^{-i\beta_n L}$, and fitting the coefficients c_n to the complex amplitude s_{int} of the propagating mode inside the delay line [20].

Surprisingly, despite the fact that the whole system is unidirectional, the schematic in Fig. 2b immediately seems to imply that an etalon-like resonance exists: light makes multiple round trips through the delay line, propagating forward through the unidirectional mode but coupling back evanescently. We also observe that the internal amplitude $|s_{\text{int}}|$ exceeds the input amplitude $|s_+|$, confirming that light makes multiple roundtrips [20]. As such, the unidirectional delay line is essentially a nonreciprocal version of a Gires-Tournois (GT) interferometer [34]. In [20] we show that these nonreciprocal resonances can also be critically coupled, and that they occur each wavelength in cavity length rather than each half-wavelength (as in a reciprocal etalon), because phase pickup only occurs in the forward direction.

To demonstrate the contribution of this exotic resonance to the dynamics of the unidirectional delay line, we use Eq. (3) to find an expression for the total group delay [20]:

$$\tau_g = \tau_j + (\tau_p + \tau_j)\Re\left(\frac{u_2}{e^{i\tau_p\omega} - u_2} + \frac{m}{m + u_2 e^{i\tau_p\omega}}\right), \tag{4}$$

where $m = u_1 u_2 - t_1^2$ and $\tau_p \approx L / v_g$ is the group delay due to the propagating mode. In the limit of long delay lines, the evanescent coupling becomes negligible and the group delay becomes equal to $\tau_0 = \tau_p + 2\tau_j$. The maximum variation in the group delay is given by

$$\tau_g^{\pm} = \tau_j + \left(\frac{1 \pm |u|}{1 \mp |u|} \right) (\tau_j + \tau_p) \approx \tau_j + \left(\frac{Q}{\omega_0 \tau_p} \right)^{\pm 1} (\tau_j + \tau_p), \quad (5)$$

where Q is the resonance quality factor in the limit that the junctions store much less energy than the propagating mode [35]. Despite not considering the dispersion of Ω, Eqs. (4),(5) are in good agreement with the numerically obtained group delay (Fig. 2d), although better for a narrowband pulse ($\Delta f = f_0 / 40$, purple dots) than for a broadband pulse ($\Delta f = f_0 / 8$, blue dots). This is because resonances at longer lengths have bandwidths narrower than the broadband pulse. We have performed the same analysis for a 1 μm dielectric layer height, obtaining similarly good agreement [20].

So far, we have investigated the dynamics of a canonical one-way system, enabling us to derive a simple analytical model predicting its main features. The practicality of this approach, however, is limited by absorption and spatial dispersion [36]. Our findings, on the other hand, generally apply to any unidirectional waveguiding system, including unidirectional edge states in photonic topological insulator (PTI) systems [37,38]. To demonstrate it, we now turn to an interface between two photonic crystals with a shared band gap at 4.2 GHz. One of the photonic crystals has a band structure with non-trivial topology, resulting in a single protected unidirectional edge state between the two crystals.

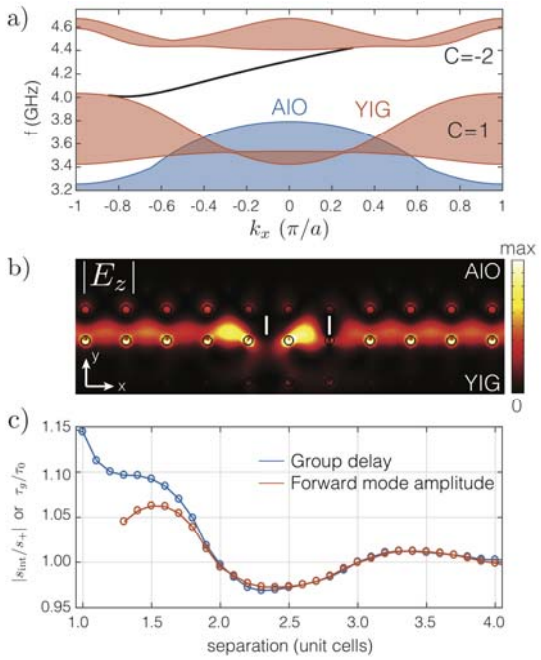

Fig. 3: a) Photonic crystal band structures and edge state dispersion (black line). C gives the Chern numbers of the two YIG crystal bands. b) Electric field amplitude of the topologically protected edge state moving around two PEC rectangles. c) Group delay enhancement and edge state amplitude between the obstacles, demonstrating the same type of nonreciprocal resonance.

The topological photonic crystal, originally described in Ref. [29], consists of a square lattice (lattice constant $a_{YIG} = 39.2$ mm) of yttrium-iron-garnet (YIG) rods ($r_{YIG} = 0.11a$) biased with a 0.16T magnetic field. The trivial photonic crystal consists of a square lattice of aluminum oxide rods ($r_{AlO} = 0.106a$, $a_{AlO} = a_{YIG}/\sqrt{2}$), rotated by 45 degrees with respect to the non-trivial crystal. The two crystals are separated by $0.75a_{YIG}$. At this interface, the topological features of the two crystals and the bulk-edge correspondence [39] ensure the presence of a robust one-way edge mode, similar to the chiral edge states in the integer quantum Hall effect [8,9]. This edge state is shown in Fig. 3a by the black line.

To excite evanescent fields and induce a delay in the signal propagation along the edge, similar to the thin channel in Fig. 1, we add two PEC barriers along the path of the edge state. Fig. 3b shows the electric field intensity of the one-way edge state as it propagates past these obstructions, demonstrating full transmission despite the presence of the scatterers. Both PEC rectangles excite evanescent modes and contribute to the group delay of an incident pulse, similar to the waveguide junctions in the previous example [20]. For close enough proximity, we anticipate that the rectangles may also interact evanescently, resulting in the exotic nonreciprocal resonant phenomenon discussed previously. Fig. 4b shows the calculated group delay for a Gaussian pulse ($f_0 = 4.2$ GHz, $\Delta f = f_0 / 20$) as a function of the separation between the two obstructions in blue. This curve is normalized to the group delay of the "uncoupled" obstructions (*i.e.* the added delay of each individual rectangle at their specific position and the propagation delay between them separately [20]). As expected, we indeed observe a clear decaying oscillation in the group delay due to the interaction between the scatterers, reminiscent of the oscillation in the delay of the plasmonic delay line. Comparing the normalized group delay to the amplitude of the edge mode itself between the two obstructions (red line), we observe a clear correlation. This corroborates the hypothesis that the variation in group delay is due to the same non-reciprocal resonance phenomenon. However, there are also fundamental differences between the two cases: for example, in the photonic crystal the Bloch wavefunction itself leads to strong variation of the group delay imparted by a single scatterer depending on the location of the scatterer inside the unit cell [20], which adds a degree of complexity. Despite these differences, the two systems we have discussed here display very similar dynamical behavior, simply as a result of their unidirectionality.

The etalon-like resonance uncovered here demonstrates that the dynamics of unidirectional waveguides may be more complicated than anticipated, but the implications may be much broader. In general, resonances lead to many desirable effects (such as enhanced light-matter interaction and delays), but they can also be undesired (*e.g.* leading to pulse shape distortion). Being aware of these resonances is important, so that potential benefits may be reaped and adverse consequences can be avoided. For example, we are currently exploring how this resonance can be utilized to create broadband topologically protected slow light [40], for which to date there is no known practical approach, but which would be of great relevance for robust delay lines [5,11]. On the other hand, the existence of this exotic resonance implies that a form of (weak) disorder induced localization could occur in unidirectional waveguides as well. Finally, it is important to note that our proposed demonstrations also work in the near-infrared, where the need for delay lines is most pressing, but with reduced unidirectional bandwidths [22,41]. A potentially more promising avenue to pursue in the near-infrared is the photonic analogue to the quantum spin Hall effect [38,42], which can arise in all-dielectric platforms, does not rely on a magnetic bias, and is therefore readily compatible with integrated photonics [43,44].

In conclusion, we have shown that unidirectional waveguides can delay a pulse by more than its temporal width in a fraction of the wavelength in a robust fashion. Due to the unidirectional nature of the waveguide, such a delay line is robust against disorder or extremely strong scatterers, guaranteeing full transmission throughout the unidirectional window. However, we have shown that only considering transmission hides rich temporal dynamics in these unidirectional systems with strong scatterers. For example, despite the absence of a backward propagating mode, resonances may arise in unidirectional

waveguides if another obstruction exists within the decay length of the backward evanescent mode. They can strongly affect the dynamics of the waveguide, enhance delay times or even distort incoming signals (while still fully transmitting). These resonances provide an additional degree of freedom in engineering the response of unidirectional waveguides, and may therefore prove highly useful for various nanophotonic applications.

References

[1] R. S. Tucker, P. Ku, and C. J. Chang-hasnain, J. Light. Technol. **23**, 4046 (2005).

[2] T. Baba, Nat. Photonics **2**, 465 (2008).

[3] M. Minkov and V. Savona, Optica **2**, 631 (2015).

[4] D. A. B. Miller, Phys. Rev. Lett. **99**, 203903 (2007).

[5] S. Hughes, L. Ramunno, J. F. Young, and J. E. Sipe, Phys. Rev. Lett. **94**, 033903 (2005).

[6] S. Mazoyer, J. P. Hugonin, and P. Lalanne, Phys. Rev. Lett. **103**, 1 (2009).

[7] S. G. Johnson, P. Bienstman, M. A. Skorobogatiy, M. Ibanescu, E. Lidorikis, and J. D. Joannopoulos, Phys. Rev. E **66**, 066608 (2002).

[8] F. D. M. Haldane and S. Raghu, Phys. Rev. Lett. **100**, 013904 (2008).

[9] S. Raghu and F. D. M. Haldane, Phys. Rev. A **78**, 033834 (2008).

[10] Z. Wang, Y. Chong, J. D. Joannopoulos, and M. Soljačić, Nature **461**, 772 (2009).

[11] M. Hafezi, E. A. Demler, M. D. Lukin, and J. M. Taylor, Nat. Phys. **7**, 907 (2011).

[12] K. Lai, T. Ma, X. Bo, S. Anlage, and G. Shvets, Sci. Rep. **6**, 1 (2016).

[13] S. A. Mann, D. L. Sounas, and A. Alù, Optica **6**, 104 (2019).

[14] J. R. Maack, N. A. Mortensen, and M. Wubs, Europhysics Lett. **119**, 17003 (2017).

[15] Ş. E. Kocabaş, G. Veronis, D. A. B. Miller, and S. Fan, Phys. Rev. B **79**, 1 (2009).

[16] R. Zia, M. D. Selker, P. B. Catrysse, and M. L. Brongersma, J. Opt. Soc. Am. A **21**, 2442 (2004).

[17] J. A. Dionne, L. A. Sweatlock, H. A. Atwater, and A. Polman, Phys. Rev. B **73**, 035407 (2006).

[18] A. R. Davoyan, I. V. Shadrivov, and Y. S. Kivshar, Opt. Express **16**, 21209 (2008).

[19] P. Lalanne, S. Coudert, G. Duchateau, S. Dilhaire, and K. Vynck, ACS Photonics **6**, 4 (2019).

[20] (n.d.).

[21] J. J. Brion, R. F. Wallis, A. Hartstein, and E. Burstein, Phys. Rev. Lett. **28**, 1455 (1972).

[22] Z. Yu, G. Veronis, Z. Wang, and S. Fan, Phys. Rev. Lett. **100**, 023902 (2008).

[23] L. Shen, Y. You, Z. Wang, and X. Deng, Opt. Express **23**, 950 (2015).

[24] M. S. Kushwaha, Surf. Sci. Rep. **41**, 1 (2001).

[25] M. S. Kushwaha and P. Halevi, Phys. Rev. B **36**, 5960 (1987).

[26] U. K. Chettiar, A. R. Davoyan, and N. Engheta, Opt. Lett. **39**, 1760 (2014).

[27] A. R. Davoyan and N. Engheta, Phys. Rev. Lett. **111**, 257401 (2013).

[28] O. Luukkonen, U. K. Chettiar, and N. Engheta, IEEE Antennas Wirel. Propag. Lett. **11**, 1398 (2012).

[29] Z. Wang, Y. D. Chong, J. D. Joannopoulos, and M. Soljačić, Phys. Rev. Lett. **100**, 013905 (2008).

[30] P. R. McIsaac, IEEE Trans. Microw. Theory Tech. **39**, 1808 (1991).

[31] C. Ernst, V. Postoyalko, and N. G. Khan, IEEE Trans. Microw. Theory Tech. **49**, 192 (2001).

[32] E. L. Ginzton, *Microwave Measurements* (McGraw-Hill Book Company, Inc., 1957).

[33] S. E. Kocabas, G. Veronis, D. Miller, and S. Fan, IEEE J. Sel. Top. Quantum Electron. **14**, 1462 (2008).

[34] F. Gires and P. Tournois, C. R. Acad. Sci. Paris **258**, 6112 (1964).

[35] P. Tournois, IEEE J. Quantum Electron. **33**, 519 (1997).

[36] S. Buddhiraju, Y. Shi, A. Song, C. Wojcik, M. Minkov, I. A. D. Williamson, A. Dutt, and S. Fan, ArXiv:1809.05100 (2018).

[37] L. Lu, J. D. Joannopoulos, and M. Soljačić, Nat. Photonics **8**, 821 (2014).

[38] T. Ozawa, H. M. Price, A. Amo, N. Goldman, M. Hafezi, L. Lu, M. Rechtsman, D. Schuster, J. Simon, O. Zilberberg, and I. Carusotto, Nat. Photonics **8**, 821 (2018).

[39] M. G. Silveirinha, Phys. Rev. X **9**, 011037 (2019).

[40] J. Guglielmon and M. C. Rechtsman, Phys. Rev. Lett. **122**, 153904 (2019).

[41] B. Bahari, A. Ndao, F. Vallini, A. El Amili, Y. Fainman, and B. Kanté, Science **358**, 636 (2017).

[42] L.-H. Wu and X. Hu, Phys. Rev. Lett. **114**, 223901 (2015).

[43] S. Barik, A. Karasahin, C. Flower, T. Cai, H. Miyake, W. DeGottardi, M. Hafezi, and E. Waks, Science **359**, 666 (2018).

[44] N. Parappurath, F. Alpeggiani, L. Kuipers, and E. Verhagen, ArXiv:1811.10739 (2018).